Evaluation of Fatigue and Permanent Deformation Properties of Several Asphalt-Aggregate Field Mixes Using Strategic Highway Research Program A-003A Equipment

JOHN HARVEY, TINA LEE, JORGE SOUSA, JIMMY PAK, AND CARL L. MONISMITH

Use of fatigue and permanent shear deformation tests, equipment, and analysis procedures developed by the Strategic Highway Research Program (SHRP) A-003A project, are investigated for their applicability for to stone matrix asphalt, recycled asphalt pavement, asphalt-rubber concrete, and large stone gradation as well as conventional asphalt-concrete mixes. Materials were collected in the field and compacted in the laboratory following SHRP A-003A rolling wheel procedures. Mixes were tested for fatigue life and flexural stiffness using controlled-strain equipment. Their permanent shear deformation resistance was evaluated using the repetitive simple shear test-constant height (RSST-CH). Results show that the tests and equipment were sensitive to each of the materials tested, and also confirm engineering expectations. Rut depth predictions were made on the basis of the RSST-CH results and a proposed method for translating the permanent shear strains and load repetitions measured by the test to field rut depths and equivalent single axle loads (ESALs). When the measured ESALs and in situ rut depths were compared with test results, the method proved to be a good predictor, although resulting predictions were often somewhat conservative because mixes in the field had aged. Analysis of fatigue and stiffness data for several hypothetical pavement cross sections applying elastic layer theory showed that ranking of mixes for fatigue life depends on the fatigue curve developed from testing, measured flexural stiffness, and properties of the underlying pavement.

Performance testing and analysis methods designed under Strategic Highway Research Program (SHRP) Project A-003A provide the means to determine the relationship between fatigue life and tensile strain, flexural stiffness, and permanent shear deformation resistance of asphalt-aggregate mixes. The most important distress mechanisms and conditions that cause fatigue cracking and permanent shear deformation now can be duplicated in the laboratory, allowing direct comparisons of the performance characteristics of various mixes for mix and pavement design, measured in fundamental engineering units, (*1–3*). Rapid evaluation of the potential of various new products and mix types can be completed in the laboratory, either, before or as a substitute for field test-section construction. This is a significant improvement because field test sections require years of monitoring before their performance can be analyzed and are subject to uncontrollable variables related to construction and the environment. The enhanced testing capability provided by SHRP A-003A equipment is especially important when asphalt modifiers such as asphalt rubber or new mix types such as stone-matrix asphalt (SMA) are outside the experience of the evaluating agency, and traditional mix evaluation testing does not provide adequate information.

Institute of Transportation Studies, University of California, Berkeley, Richmond Field Station, 1301 South 46th Street, Building 452, Richmond, California 94804.

At this time, elements of the SHRP A-003A permanent deformation analysis system are being considered for inclusion in SuperPave.

STUDY OBJECTIVES

The first objective of the study was to test a variety of conventional and new materials under similar conditions for fatigue, flexural stiffness, and permanent shear deformation, to demonstrate the sensitivity of the SHRP A-003A equipment and its ability to directly compare each material's relative performance. The second objective was to use permanent shear deformation test results, together with a proposed method for predicting field rut depth, for comparison with rut depths and ESALs measured in the field. The third objective was to demonstrate the use of strain-fatigue-life relationships developed from testing in predicting fatigue life for several pavement cross sections.

MATERIALS AND TEST METHODS

Field mixes were collected during construction from two test section locations: Interstate 40, approximately 40 mi east of Barstow, California, and Interstate 45, in Waukesha County, Wisconsin. Field cores were collected on some sections both inside and outside the wheel path at times ranging from 5 to 22 months after construction.

Barstow Test Section Descriptions

Barstow sections were constructed in April 1992, and field cores were taken in September 1992. A total of 520,000 equivalent single axle loads (ESALs) was measured at the test sections during the 5 months between construction and coring.

Surface materials, including virgin asphalt concrete, asphalt-rubber concrete (RAC), and a blend of virgin and recycled asphalt pavement (RAP), were constructed in layers 60 mm (0.2 ft) thick. A large stone material was used in a 120 mm (0.4 ft) base layer below a surface 60 mm (0.2 ft) thick. Two SMA materials, with asphalt-rubber and polyolefin-modified binders, were placed as 45-mm (0.15-ft) surface layers.

Wisconsin Test Section Descriptions

One SMA mix was constructed with a polyolefin-modified binder at the Wisconsin test section. This section was constructed in June 1991 and cored in April 1993. Approximately 128,000 ESALs passed across the design lane during those 22 months.

Materials Descriptions

A partially crushed gravel was used for the Barstow mixes, whereas a completely crushed limestone was used for the Wisconsin SMA. Job mix formulas for all mixes are shown in Table 1. Typical quality assurance results for some mixes are shown in parentheses.

Specimen Preparation

The rolling wheel compaction method of University of California at Berkeley was used for the preparation of all laboratory specimens (*3,4*). Mixes were collected in the field directly in front of the paver. They were compacted in the laboratory in 20-kg (44-lb) ingots, which provided either three permanent deformation cores or one core and two fatigue beams (*1*).

After compaction, the ingots were allowed to cool overnight. Cylinders for permanent deformation testing were cored and cut to cores 15 cm (6 in.) in diameter by 5 cm (2 in.) high. Fatigue beams were cut to 5 cm by 5.25 cm by 38 cm (2 in. by 2.5 in. by 15 in).

Air-void contents were measured with parafilm (*5*). Specimens were compacted to the field air-void contents, which were measured at the time of construction and at the time of coring. Air-void contents ranged between 2 and 13 percent, depending on the mix.

Test Methods

To evaluate the specimens, two types of tests were performed: the repetitive simple shear test—constant height (RSST-CH), and the controlled-strain flexural beam fatigue test. Both tests use computer-operated, closed-loop, digital systems that control hydraulic actuators.

Repetitive Simple Shear Test—RSST-CH

All RSST-CH results were obtained with the universal testing machine (*1,6*). Tests on the laboratory specimens were performed at 60°C (140°F). Tests on field cores were performed at the maximum average 7-day pavement temperature at a depth of 50 mm (2 in.) and calculated using the method of Solaimanian and Kennedy (*7*). The temperatures were 57°C (135°F) for Barstow, California, and 43°C (109°F) for Waukesha County, Wisconsin.

For the RSST-CH, one LVDT is attached to the top and bottom platens along the vertical axis to allow the machine to maintain a constant specimen height and another is attached to the side of the core so that horizontal (shear) displacement can be measured. The shear stress was 68.9 kPa (19 psi), applied as a haversine wave with a 0.1-sec load time and a 0.6-sec rest period. Failure was defined as 5.0 percent permanent shear strain. Results for cores that did not reach failure because of time constraints were extrapolated.

Flexural Beam Fatigue Test—Controlled Strain

To determine the fatigue and stiffness characteristics of each mix, a controlled-strain flexural beam test with a third-point loading system was used (*2*). All tests were performed at 20°C (68°F) using a 10 Hz frequency sine wave. During the test, stiffness was recorded at various time intervals. Initial stiffness was defined as that occurring at the fiftieth load repetition. Fatigue failure was defined as a 50 percent reduction in stiffness.

TABLE 1 Job Mix Formulas and In Situ Quality Control Data

Section:	503	504,507	513,514	519	521	522	WIS
Material:	30% RAP 70 % Virg AC	19 mm MSA Virgin AC	19 mm MSA Asph-Rubber	38 mm MSA Base	SMA Asph-Rubber	SMA Polyolefin	SMA Polyolefin
% Passing Sieve (mm)	Job Mix Formulas (Actual in parentheses)						
38	-	-	-	100 (100)	-	-	-
25	100 (100)	100 (100)	100	95 (87)	100 (100)	100	-
19	98 (97)	99 (97)	98	75 (86)	99 (100)	99 (100)	100
9.5	63 (71)	67 (71)	64	62 (64)	74 (80)	75 (80)	70
4.75	46 (53)	50 (54)	36	48 (47)	31 (37)	29 (31)	28
2.36	36 (42)	40 (42)	20	-	23 (25)	24 (23)	20
0.60	20 (24)	21 (22)	13	21 (20)	12 (13)	16 (14)	14
0.075	4.1 (8)	4.8 (5)	4.0	5.0 (4)	4.0 (6)	8.8 (6)	10.0
Binder Content*	3.8	5.3 (5.2)	7.5	5.1 (5.1)	6.8 (5.0)	6.0 (5.2)	6.0
	*percent by wt of aggregate						
Binder	AR-4000	AR-4000	AR-4000 plus rubber	AR-8000	AR-4000 plus rubber	AR-4000 plus polyolefin	85/100 pen plus polyolefin

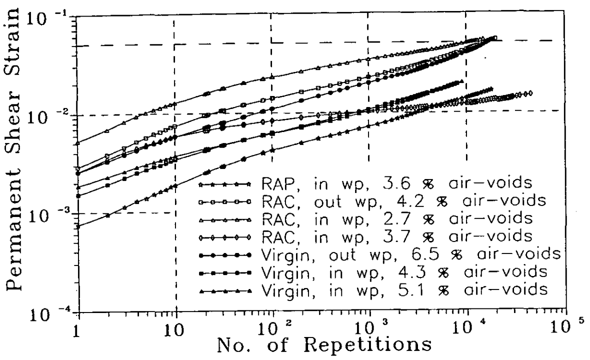

FIGURE 1 Barstow field cores RSST-CH plots, 57°C (135°F).

RSST-CH with Confinement

To evaluate the effects of confining pressure on RSST-CH, results were also obtained for field cores of two mixes from Oregon, one open graded and the other dense graded. The only difference in test method was the application of a 68.9 kPa (10 psi) confining pressure, which was applied using a membrane.

DISCUSSION OF RESULTS

Permanent Shear Deformation

Field Cores

The set of Barstow field core test results performed at 57°C (135°F) is plotted in Figure 1, and the number of RSST-CH repetitions to a 5.0 percent permanent shear strain (pss) are presented in Table 2. It can be seen that the cores from inside the wheel path had slightly lower air-void contents than those taken from outside the wheelpath and had much more permanent deformation resistance. This indicates that besides aging, which doubled the stiffness of the conventional binder in the first 5 months after construction (*8*), densification and aggregate orientation induced by traffic greatly improved permanent shear deformation resistance. Results from the limited number of cores indicate that traffic compaction improved the performance of the RAC more than it did the virgin asphalt concrete.

The Wisconsin field core test results, performed at 43°C (109°F), did not follow the expected pattern of better permanent shear deformation resistance and lower air-void contents inside the wheel path, as can be seen from the plotted results in Figure 2 and related data presented in Table 2. High air-void content and the resultant lower permanent shear deformation resistance of the core taken from within the wheelpath may not be typical.

Laboratory Specimens

RSST-CH results for all laboratory specimens tested at 60°C (140°F) are presented in Figure 3 and Table 3.

Note that the Wisconsin SMA performed very well when compacted to approximately 4.8 percent air voids but did considerably worse when compacted to 6.3 percent. The latter air-voids content was approximately the lowest air-void content achieved in the field on that project. All of the laboratory SMA specimens had a wide range of performance, depending on material type and air-void con-

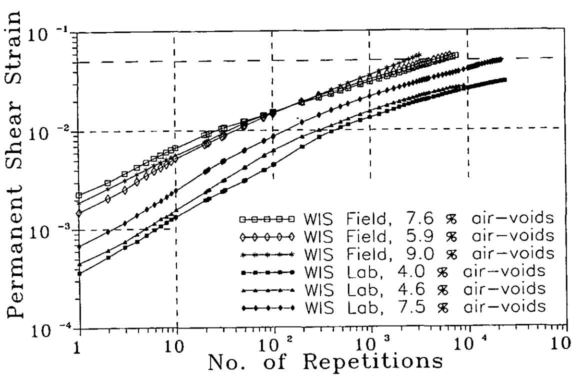

FIGURE 2 Wisconsin SMA field cores and laboratory specimens RSST-CH plots, 43°C (109°F).

TABLE 2 Repetitions to 5 Percent RSST-CH Shear Strain, Field Cores

Specimen	Material	AV	Wheelpath Location	Age	ESALS at Coring	RSST-CH Reps to 5 % Shear Strain
Barstow, Tested at 57 C (134 F)						
B60	Virgin AC	5.1	in	5 mos	520,000	176,523
B59	Virgin AC	4.3	in	5 mos	520,000	151,910
B58	Virgin AC	6.5	out	5 mos	520,000	16,578
B48	RAC	3.7	in	5 mos	520,000	42,539,242
B45	RAC	4.2	out	5 mos	520,000	16,132
B4	RAP	3.6	in	5 mos	520,000	903,134
Wisconsin, Tested at 43 C (109 F)						
WISF6	SMA polyolefin	9.0	in	22 mos	128,000	2,504
WISF5	SMA polyolefin	5.9	out	22 mos	128,000	4,621
WISF3	SMA polyolefin	7.6	out	22 mos	128,000	5,515

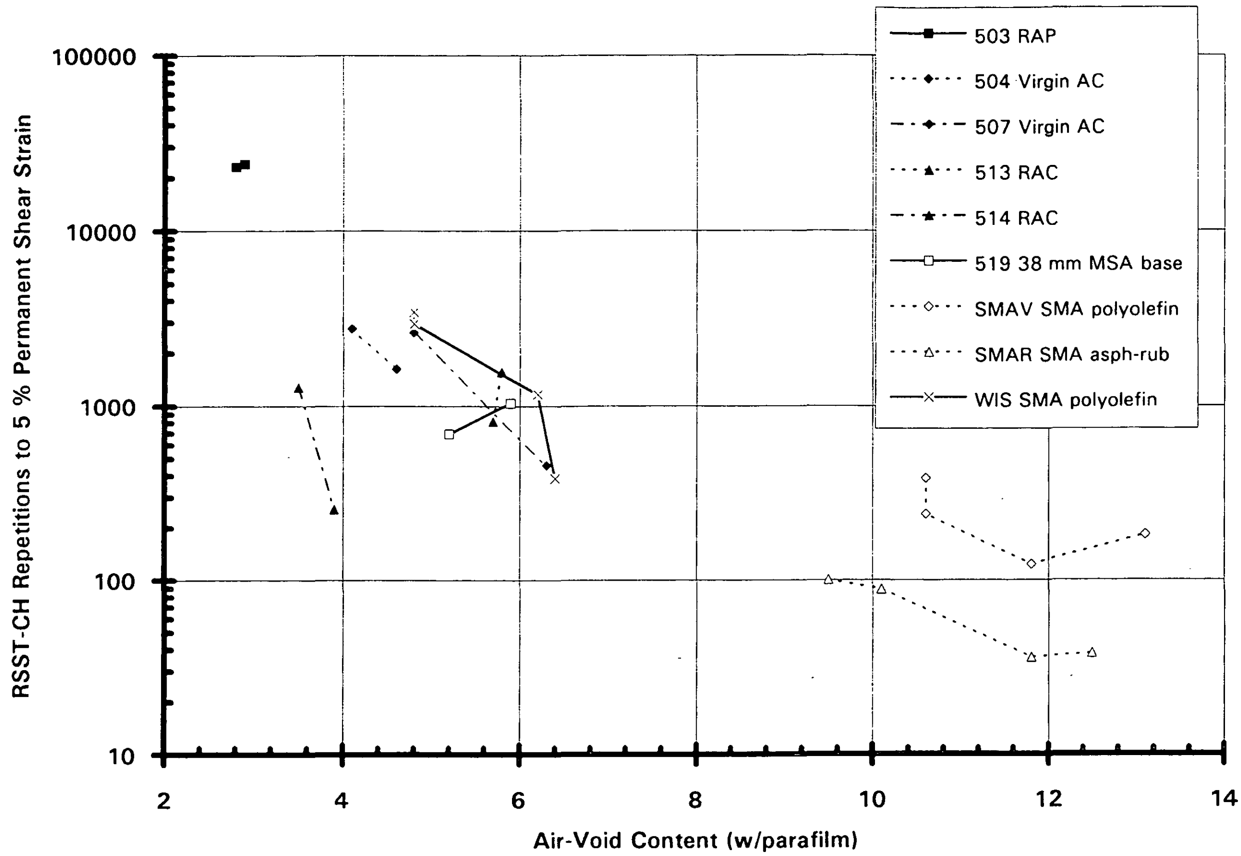

FIGURE 3 Laboratory specimens, RSST-CH repetitions to 5 percent permanent shear strain and air-void content for all mixes, 60°C (140°F).

tent. The Wisconsin SMA, which had lower air-void contents, performed better than did the Barstow SMAs, both of which had relatively low fines contents for this type of mix.

For the Barstow mixes, performance ranking followed the air-void contents, with the exception of the RAC from Section 514. This indicates the tremendous importance of compaction in achieving good permanent shear deformation resistance. Compaction can come from either construction or trafficking, but better compaction in construction will reduce the rut depth caused by densification and also reduce the susceptibility to fatigue and environmental damage before traffic densification. The study results also indicate that at 60°C (140°F) the various mixes used at the Barstow sections were not considerably different from each other with respect to the permanent shear deformation performance of non–long-term aged and laboratory-compacted mixes. However, binders may have different aging rates and varying responses to traffic compaction, which can produce larger differences in performance, such as those seen in the limited field core data already presented, and in a broader comparison of field core data from the Barstow test sections (*8*).

Several Wisconsin SMA laboratory specimens were also tested at 43°C (109°F). It can be seen in Figure 2 and Table 3 that at this temperature permanent shear deformation performance was much better than at the higher temperature. It can also be seen that the laboratory specimens performed better than the field cores. This may be in part the result of the somewhat lower air-voids contents of the laboratory cores. Aging of the binder should not have been significant in Waukesha County, Wisconsin, and little increase in permanent shear deformation resistance from aging was expected in the field cores.

Effect of Confinement on RSST-CH

Comparison of RSST-CH results, unconfined and with 68.9 kPa (10 psi) confining pressure, on duplicate cores of open-graded and dense-graded asphalt-concrete showed virtually no difference between the two testing conditions. On the basis of these tests, it was decided that confinement would not be used for the RSST-CH.

The confinement that resists permanent shear deformation during the RSST-CH is developed within the material by interparticle contact. Because the specimen is maintained at a constant height, aggregate within specimens with good interparticle contact develop dilation pressures as the aggregates attempt to move past each other under 68.9 kPa (10 psi) shear stress. This mechanism appears to be more important than the confining stress applied. Confining pressures greater than 68.9 kPa (10 psi) may influence RSST-CH results, but they were not investigated in this study.

Some lateral densification of the open-graded specimens was observed after the confining stress was applied, but maintenance of a constant height prevented axial densification, and the epoxy fastening the specimen to the platens prevented lateral densification at the ends of the specimens.

TABLE 3 Repetitions to 5 Percent RSST-CH Shear Strain, Laboratory Specimens

Specimen	Material	AV	RSST-CH Reps to 5 % Shear Strain
Tested at 60 C (140 F)			
503-N1	RAP	2.8	23064
503-N3	RAP	2.9	24030
average		*2.9*	*23547*
504-N1-3	Virgin AC	4.1	2780
504-N1-1	Virgin AC	4.6	1632
average		*4.4*	*2206*
507-N1	Virgin AC	4.8	2635
507-N2	Virgin AC	6.3	457
average		*5.6*	*1546*
513-N1C	RAC	5.7	817
513-N1-A	RAC	5.8	1569
average		*5.8*	*1193*
514-N4-B	RAC	3.5	1281
514-N3-A	RAC	3.9	257
average		*3.7*	*769*
519-N1	38mm MSA base	5.2	691
519-N4	38mm MSA base	5.9	1033
average		*5.6*	*862*
SMAV-2-1	SMA polyolefin	10.6	385
SMAV-6	SMA polyolefin	10.6	240
SMAV-1-1	SMA polyolefin	11.8	123
SMAV-4	SMA polyolefin	13.1	182
average		*11.5*	*233*
SMAR-6	SMA rubber	9.5	101
SMAR-2-1	SMA rubber	10.1	89
SMAR-4	SMA rubber	11.8	36
SMAR-7	SMA rubber	12.5	38
average		*11.0*	*66*
WIS 2-1	SMA polyolefin	4.8	3457
WIS 2-2	SMA polyolefin	4.8	2953
WIS 4	SMA polyolefin	6.2	1163
WIS 3-1	SMA polyolefin	6.4	385
average		*5.6*	*1990*
Tested at 43 C (109 F)			
WIS 1-1	SMA polyolefin	4.0	71250
WIS 2-3	SMA polyolefin	4.6	312666
WIS 5	SMA polyolefin	7.5	24062
average		*5.4*	*135993*

Fatigue and Flexural Stiffness

Flexural Stiffness

Initial flexural stiffness results are summarized in Table 4. The RAP material had the highest stiffness, most likely because of the air-void content, the presence of very hard binder material from the recycled pavement, and the addition of only 3.8 percent virgin asphalt cement (by weight of aggregate). Note that the 1.5 Maximum-Size Aggregate (MSA) base material contained a nominally stiffer asphalt, AR-8000, but still exhibited less stiffness than the virgin asphalt mix that contained AR-4000. This is most likely because of

TABLE 4 Fatigue Beam Test Results, All Materials

Tested at 20 C (67 F)										
Material	Specimen	AV	Strain (micro-strain)	Initial (MPa)	Stiffness (psi)	Nf Repetitions to Failure (50 percent initial stiff.)	Total Dissipated Energy (psi)	Regression Equation Nf=k1(strain)^k2 k1	k2	R^2
503 RAP	503-N1-A	2.6	500	6,136	890,495	36,622	1,900			
	503-N1-3	3.9	400	6,323	917,705	73,053	2,414			
	503-2B	2.6	250	6,370	924,559	431,764	5,708			
	503-N3-B	2.8	250	6,083	882,840	459,878	4,985			
average		*3.0*		*6,228*	*903,900*		constants:	2.86E-08	-3.66	0.998
507 Virgin	507-N1-A	5.2	400	3,910	567,521	350,068	14,943			
	507-N2-A	5.1	350	3,318	481,579	149,999	2,520			
	507-N1-B	3.7	550	4,054	588,333	26,298	1,471			
	507-N2-B	5.8	600	3,132	454,553	39,494	2,020			
average		*5.0*		*3,603*	*522,997*		constants:	8.45E-09	-3.90	0.697
514 RAC	514-N1-A	3.5	350	2,957	429,157	190,562	5,166			
	514-N3-B	3.6	300	2,989	433,835	574,923	11,798			
	514-N1-B	3.1	600	2,809	407,672	48,341	4,282			
	514-N3-A	3.9	400	2,746	398,494	183,289	6,985			
average		*3.5*		*2,875*	*417,290*		constants:	1.04E-06	-3.30	0.939
519 38mm	519-N2-A	7.3	300	3,696	536,375	3,308,566	15,570			
MSA base	519-N4-B	6.3	250	3,207	465,468	1,008,293	7,155			
	519-N3-A	7.2	400	2,316	336,176	43,139	673			
	519-N4-A	6.3	400	3,141	455,904	49,169	1,123			
average		*6.8*		*3,090*	*448,481*		constants:	3.29E-23	-8.03	0.724
SMAV	SMAV-4A	11.0	400	1,986	288,268	150,000	3,756			
polyolefin	SMAV-4B	10.8	400	2,537	368,212	97,047	1,649			
	SMAV-5A	11.0	200	2,724	395,424	1,003,047	4,903			
	SMAV-7A	10.6	250	2,845	412,921	2,629,080	10,974			
	SMAV-2B	11.1	300	2,411	349,915	175,000	2,051			
average		*10.9*		*2,501*	*362,948*		constants:	8.21E-09	-3.87	0.681
SMAR	SMAR-1B	10.4	450	1,512	219,439	15,000	487			
a-rubber	SMAR-4A	10.6	400	1,745	253,336	75,923	913			
	SMAR-2A	10.8	300	2,014	292,283	316,536	4,726			
	SMAR-2B	10.2	300	2,052	297,782	227,992	1,813			
average		*10.5*		*1,831*	*265,710*		constants:	7.54E-18	-6.41	0.920
WIS	WIS-3-2	5.0	700	5,401	783,864	25,000	5,020			
SMA	WIS-4A	5.4	250	6,541	949,371	1,134,037	23,846			
polyolefin	WIS-4B	7.1	400	5,278	766,045	262,957	9,598			
average		*5.8*		*5,740*	*833,093*		constants:	4.97E-08	-3.72	0.993

the lower air-void contents of the virgin asphalt specimens, although the two asphalt cements may have different temperature susceptibilities and therefore similar stiffness at 20°C (67°F). The inclusion of rubber in the AR-4000 asphalt used for the asphalt rubber material reduced stiffness by approximately 20 percent compared with the virgin asphalt material, despite somewhat lower air-void contents.

Fatigue

The relationships of controlled-strain fatigue versus strain are plotted in Figure 4, and test results are included in Table 4. The equations were obtained from least-squares regression of the fatigue beam test data and are of the form

$$Nf = k1 * (\text{strain})^{k2}$$

where

Nf = repetitions to a 50 percent reduction in stiffness,
strain = average strain used throughout the test, and
$k1$ and $k2$ = constants.

Although three to five beams were tested for each material, four being the minimum recommended for defining a fatigue curve (*9,2*), the results provide insight into the behavior of the various materials. In particular, it can be seen that the Barstow large-stone base and SMA with asphalt rubber had higher exponent values ($k2$). The plotted fatigue equations cross each other and reverse the fatigue-life rankings of the mixes between 200 and 500 microstrain.

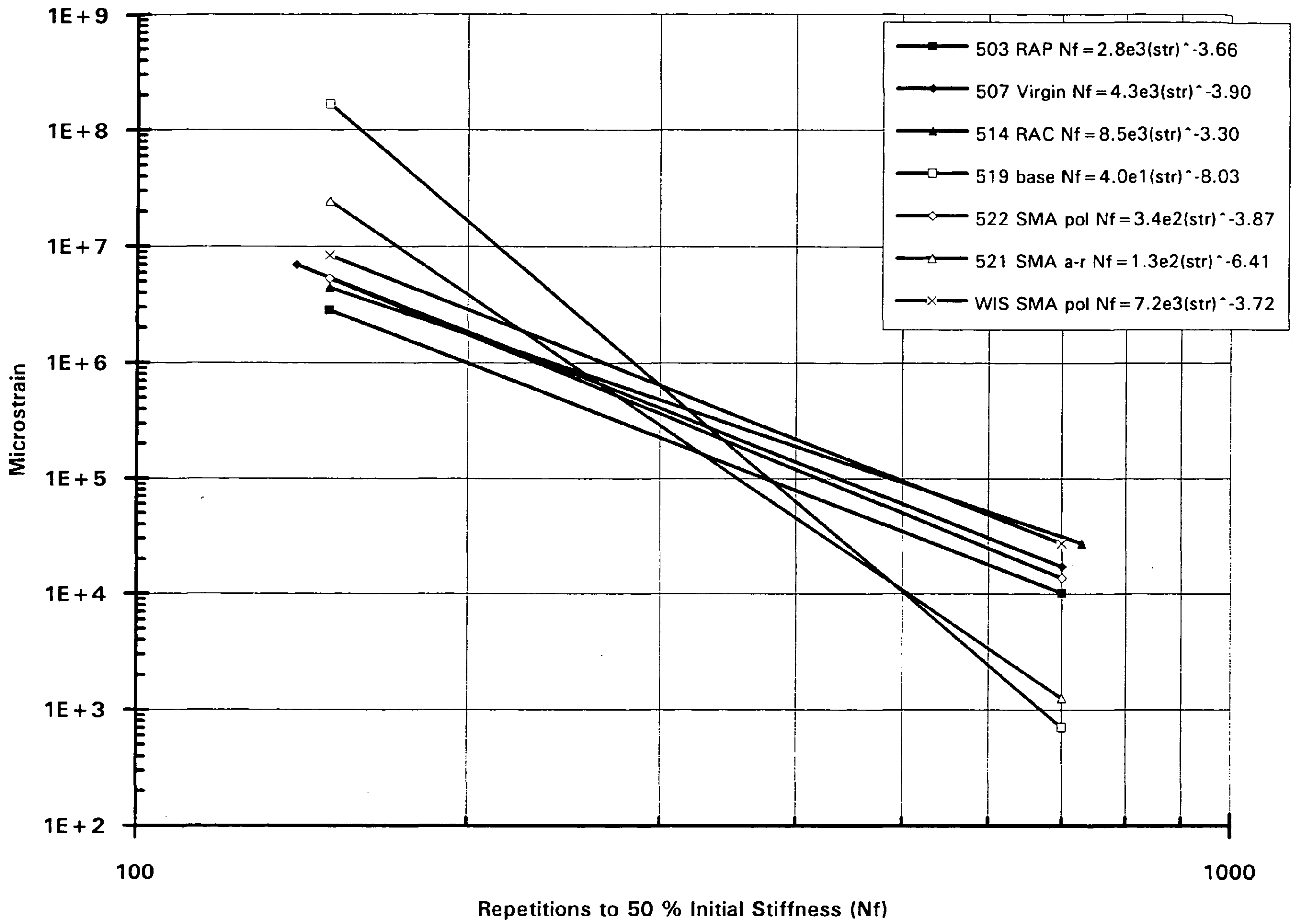

FIGURE 4 Controlled-strain fatigue life equations for all materials, 20°C (67°F).

It can be seen that total dissipated energy for each mix follows fatigue life (Table 4). Evaluation of fatigue performance in terms of total dissipated energy offers no advantages at this time.

PERFORMANCE PREDICTION ANALYSIS

To examine possible uses for the mix performance test data presented above, beyond performance ranking, performance prediction analyses were executed. The methods presented here are still being developed and require further validation; however, results are indicative of the information that can be obtained.

Permanent Deformation Performance Prediction

The following equations presented in a paper by Sousa and Solaimanian (*10*) were used to predict rut depths based on test data previously presented.

$$\text{Field Rut Depth (in.)} = 11 * \text{pss} \quad (1a)$$

$$\text{Field Rut Depth (mm)} = 280 * \text{pss} \quad (1b)$$

where pss is the permanent shear strain measured using the RSST-CH.

$$\log(\text{RSST-CH reps}) = -4.36 + 1.240 \log(\text{ESAL}) \quad (2)$$

where RSST-CH reps is the number of 68.9 kPa (10 psi) load repetitions to a given shear strain (pss) using the RSST-CH, and ESAL is the corresponding equivalent single axle loads.

Using Equation 1, a 5 percent permanent shear strain (pss) selected as failure for comparison of the relative performance of the materials corresponds to a 14-mm (0.55-in.) rut depth (Table 3). Other rut depths can be selected, depending on performance specifications for a given project.

The RSST-CH repetitions to ESALs shift factor are based on correlation of results from SHRP General Pavement Sections that were 1 to 10 years old and account for traffic wander (*10*). The permanent shear strain to field rut depth shift factor is based on finite element analysis (*11*). Additional data, including that presented in this paper, are in agreement with this performance prediction analysis method; additional field validation data may further refine the two shift factors.

For comparison with field rut depth measurements, ESALs measured using weigh-in-motion equipment at the test sections between construction and rut depth measurement were converted to RSST-CH repetitions using Equation 2. The results were: Barstow, 520,000 ESALs corresponding to 534 RSST-CH repetitions, and Wisconsin, 128,000 ESALs corresponding to 94 RSST-CH repetitions. Permanent shear strain for the appropriate RSST-CH repetitions for each test then was found. Permanent shear strains study for the field cores included in this are found (in Figures 1 and 2). Equation 1 was used to convert permanent shear strains to corresponding rut depths; results of these calculations are in Table 5 for the field cores and in Table 6 for the laboratory specimens.

For the Barstow specimens, rut depths predicted using field cores are lower than those predicted using laboratory specimens and are closer to the actual field rut depths. This can be attributed to binder hardening (aging) caused by extreme temperatures at the Barstow site that the in situ pavement and field cores both were subjected to. Long-term oven-aging of the laboratory specimens before testing would provide a less conservative estimate of field performance.

The Wisconsin section, which was subjected to lower temperatures and therefore less binder aging than the Barstow site, had field rut depths similar to those predicted from the field and laboratory specimens.

A previous study (*3*) indicates that Texas gyratory compaction specimens have less permanent shear deformation resistance, as measured using the RSST-CH, than do rolling wheel specimens. Thus, it would be expected that the predicted rut depths obtained from rolling wheel specimens in this study would be greater, and therefore even more conservative, if the field mixes had been compacted using a gyratory device.

Although large rut depths are predicted by the test results for the Barstow SMAs, the fact that the lift thickness is only about 45 mm (1.8 in.) means that this material will not be subjected to critical shear forces in the field. Critical shear forces have been found by finite element analysis to generally occur near the edge of the tire, at a depth of approximately 50 mm (2 in.). The effects of confining forces from the underlying, less rut-susceptible material just below the SMA on these sections will tend to reduce the actual shear deformations (S. Weissman and C. L. Monismith, unpublished data). For this reason, little or no permanent shear deformation should occur in these materials in the field, as was observed by the field crew during coring.

ANALYSIS OF FATIGUE TEST RESULTS

To evaluate the anticipated fatigue performance of a mix, the effects of both stiffness and the strain-fatigue life curve must be included in a mechanistic analysis of the pavement. For the mixes included in this study, eight pavement cross sections were used that cover a fairly wide range of cases. Cross sections included 50 mm and 100 mm (2 in. and 4 in.) overlays, thick and thin underlying pavement structures, and cracked and uncracked underlying asphalt-concrete layers, as is illustrated in Figure 5.

For each cross section and mix stiffness, the principal tensile strain at the bottom of the overlay was calculated using ELSYM5 elastic layer analysis. The anticipated repetitions to failure for each case were then determined using the calculated principal tensile strain and the strain-fatigue relationships that resulted from testing, as represented in Figure 4 and Table 4. These results, and the ranking of the mixes for fatigue life for each pavement cross section, are summarized in Table 7.

The ranking of the mixes varies widely, depending on the combination of the strength of the underlying pavement, stiffness of the overlay material, and fatigue life-strain equation found for each overlay material from beam testing. For example, for all pavements with uncracked underlying asphalt-concrete, those with a 100-mm

TABLE 5 Comparison of Predicted and Measured Field Rut Depths, Field Cores

Spec	Material	AV	Wheelpath Location	Age at Coring	Rut Depth Predicted from RSST-CH (mm)	Average Field Rut at Coring * (mm)	Maximum Field Rut at Coring * (mm)
Tested at 57 C (134 F)							
B60	Virgin AC	5.1	in *	5 mos	2.5	0.7	1.2
B59	Virgin AC	4.3	in *	5 mos	2.6	0.7	1.2
B58	Virgin AC	6.5	out	5 mos	4.7	0.7	1.2
B48	RAC	3.7	in *	5 mos	2.7	1.0	1.8
B45	RAC	4.2	out	5 mos	5.5	1.0	1.8
B4	RAP	3.6	in *	5 mos	1.7	0.6	0.9
Tested at 43 C (109 F)						**	**
WISF6	SMA polyolefin	9.0	in **	22 mos	4.1	1.0	2.3
WISF5	SMA polyolefin	5.9	out	22 mos	4.0	1.0	2.3
WISF3	SMA polyolefin	7.6	out	22 mos	4.1	1.0	2.3

* After 520,000 ESALs, equiv. to 534 RSST-CH reps

** After 128,000 ESALs, equiv. to 94 RSST-CH reps

TABLE 6 Comparison of Predicted and Measured Field Rut Depths, Laboratory Specimens

Spec	Material	AV	Rut Depth Predicted from RSST-CH (mm) *	Average Field Rut at Coring (mm) *	Maximum Field Rut at Coring (mm) *
Tested at 60 C (140F)					
503-N1	RAP	2.8	3.8	0.6	0.9
503-N3	RAP	2.9	4.5	0.6	0.9
504-N1-3	Virgin AC	4.1	8.3	0.7	1.2
504-N1-1	Virgin AC	4.6	9.5	0.7	1.2
507-N1	Virgin AC	4.8	9.6	0.7	1.2
507-N2	Virgin AC	6.3	14.9	0.7	1.2
513-N1C	RAC	5.7	12.8	1.0	1.8
513-N1-A	RAC	5.8	10.8	1.0	1.8
514-N4-B	RAC	3.5	11.9	1.0	1.8
514-N3-A	RAC	3.9	17.2	1.0	1.8
519-N1	1.5 inch	5.2	13.0	na	na
519-N4	1.5 inch	5.9	11.6	na	na
SMAV-2-1	SMA polyolefin	10.6	16.2	na	na
SMAV-6	SMA polyolefin	10.6	17.0	na	na
SMAV-1-1	SMA polyolefin	11.8	22.2	na	na
SMAV-4	SMA polyolefin	13.1	19.6	na	na
SMAR-6	SMA a-rubber	9.5	25.1	na	na
SMAR-2-1	SMA a-rubber	10.1	24.2	na	na
SMAR-4	SMA a-rubber	11.8	42.7	na	na
SMAR-7	SMA a-rubber	12.5	33.2	na	na
		* After 520,000 ESALs, equiv. to 534 RSST-CH reps			
Tested at 43 C (109 F)					
WIS 2-3	SMA polyolefin	4.8	1.2	1.0	2.3
WIS 1-1	SMA polyolefin	4.8	1.7	1.0	2.3
WIS 5	SMA polyolefin	6.4	2.3	1.0	2.3
		* After 128,000 ESALs, equiv. to 94 RSST-CH reps			

(4-in.) overlay on thick pavements with cracked underlying asphalt-concrete, and those in which lower tensile strains would be expected at the bottom of the overlay, the 38-mm (1.5-in.) MSA base material had the greatest fatigue life. It can be seen in Figure 4 that this material has the best fatigue performance for low strain levels (below 300 microstrain). The same mix ranked fifth or sixth for the less substantial pavement structures. The Wisconsin SMA material was ranked first or second for all cases in which the underlying asphalt-concrete was cracked, which would be expected from its high stiffness (Table 4), which would tend to limit strains, and good fatigue performance at high strain levels (Figure 4).

The reliability of the fatigue curves presented must be considered when evaluating the rankings of the mixes for this study. In general, regression coefficients are high (Table 4), indicating good reliability. For those mixes with low regression coefficients, more beams would have been tested if sufficient material had been available.

Evaluation of the variance and the associated calculation of reliability for the experiment designs used here (three to five beams at two or three strain levels) has been presented by Deacon et al. (*9*). In the same report, data are presented indicating preliminary shift factors for converting fatigue beam repetitions to ESALs for different levels of in situ pavement cracking.

CONCLUSIONS AND RECOMMENDATIONS

The following conclusions and recommendations were drawn from the results presented in this paper:

- The kind of performance prediction analysis performed for this paper cannot be obtained using traditional mix design testing and analysis (i.e., Marshall and Hveem methods). In particular, tradi-

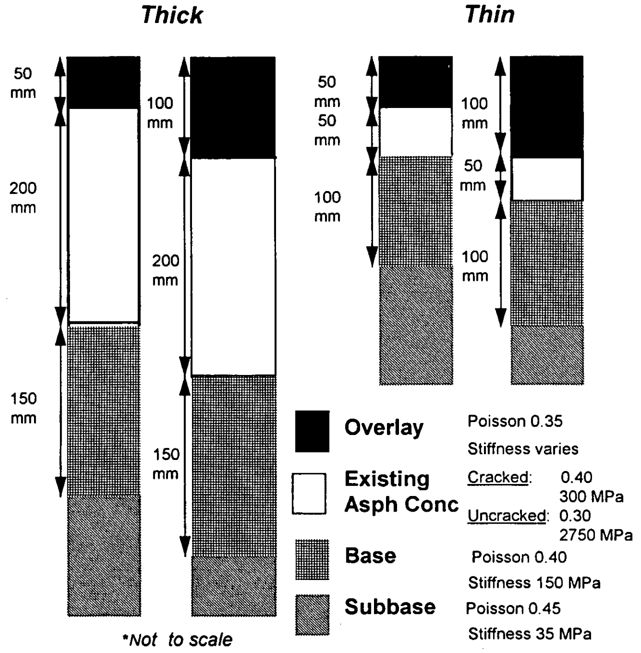

FIGURE 5 Pavement cross sections used for analysis of fatigue life.

tional mix design testing and evaluation methods allow little analysis beyond checking for minimum air-void content under standard compaction for non-conventional mixes, such as RAC and SMAs, let alone comparisons of predicted performance for conventional and nonconventional mixes.

The SHRP A-003A performance-based mix tests used in this study to evaluate permanent deformation and fatigue properties, the RSST-CH, and fatigue beam test, respectively, are sensitive to and reproducible for both conventional and nonconventional asphalt-aggregate mixes. In this study, the tests were sensitive to SMA mixes with polyolefin-modified binders and asphalt-rubber binder, dense-graded, asphalt-rubber mixes, conventional asphalt-concrete, RAP, and 38-mm (1.5-in.) MSA base material. All results followed engineering expectations and past experience and correlated with applicable field results.

- Inclusion of three different SMA mixes, all from field test sections, permitted evaluation of the sensitivity of SMA performance to several mix variables. In particular, it showed that SMA performance for both permanent shear deformation and fatigue depends on both the design and construction of the mix, and that SMA performance can be better (Wisconsin SMA) or worse (Barstow SMAs) than alternative mixes. The same can be said for any mix, including all of those evaluated in this study. There is no mix type, binder or aggregate, that cannot be made very good or very bad by the mix design or construction.

TABLE 7 Ranking of Mixes for Fatigue Life for Various Pavement Structures

Rank	Thick Pavement Uncracked Existing AC 50 mm Overlay	Thick Pavement Uncracked Existing AC 100 mm Overlay	Thin Pavement Uncracked Existing AC 50 mm Overlay	Thin Pavement Uncracked Existing AC 100 mm Overlay
1	519 38mm MSA base	519 38mm MSA base	519 38mm MSA base	519 38mm MSA base
Nf	6.05E+10	1.57E+12	1.76E+08	1.51E+09
2	503 30 % RAP	507 Virgin AC	WIS SMA polyolefin	507 Virgin AC
Nf % of # 1	0.39	0.07	12.3	1.2
3	WIS SMA polyolefin	SMAR SMA asph-rubber	507 Virgin AC	SMAR SMA asph-rubber
Nf % of # 1	0.32	0.06	7.9	1.1
4	507 Virgin AC	WIS SMA polyolefin	503 30 % RAP	SMAV SMA polyolefin
Nf % of # 1	0.29	0.04	7.5	0.9
5	SMAR SMA asph-rubber	503 30 % RAP	514 Asphalt-rubber	514 Asphalt-rubber
Nf % of # 1	0.19	0.03	2.0	0.7
6	SMAV SMA polyolefin	SMAV SMA polyolefin	SMAV SMA polyolefin	WIS SMA polyolefin
Nf % of # 1	0.10	0.02	1.4	0.6
7	514 Asphalt-rubber	514 Asphalt-rubber	SMAR SMA asph-rubber	503 30 % RAP
Nf % of # 1	0.07	0.01	0.5	0.4

Rank	Thick Pavement Cracked Existing AC 50 mm Overlay	Thick Pavement Cracked Existing AC 100 mm Overlay	Thin Pavement Cracked Existing AC 50 mm Overlay	Thin Pavement Cracked Existing AC 100 mm Overlay
1	SMAV SMA polyolefin	519 38mm MSA base	WIS SMA polyolefin	WIS SMA polyolefin
Nf	6.78E+05	2.35E+06	1.52E+05	7.48E+05
2	WIS SMA polyolefin	WIS SMA polyolefin	514 Asphalt-rubber	503 30 % RAP
Nf % of # 1	75.4	84.0	56.0	63.8
3	507 Virgin AC	503 30 % RAP	507 Virgin AC	507 Virgin AC
Nf % of # 1	48.7	57.8	51.6	44.7
4	503 30 % RAP	507 Virgin AC	503 30 % RAP	514 Asphalt-rubber
Nf % of # 1	43.7	48.9	51.4	32.4
5	514 Asphalt-rubber	514 Asphalt-rubber	SMAV SMA polyolefin	519 38mm MSA base
Nf % of # 1	42.2	30.1	24.1	23.1
6	519 38mm MSA base	SMAV SMA polyolefin	519 38mm MSA base	SMAV SMA polyolefin
Nf % of # 1	33.6	20.1	7.8	15.8
7	SMAR SMA asph-rubber	SMAR SMA asph-rubber	SMAR SMA asph-rubber	SMAR SMA asph-rubber
Nf % of # 1	11.3	10.0	5.2	3.6

• From the previous conclusions, the critical need for performance-based tests and analysis, such as those used for this study, is obvious. Without them, there are too many possible combinations of aggregate, binder, modifier, gradation and binder content, and in situ conditions (temperature, existing pavement, etc.) to estimate in situ mix performance with adequate precision to be able to determine the most cost-effective mix for a given project.

• Effects of aging and traffic densification on permanent shear deformation resistance were demonstrated. To improve the rut depth and fatigue life predictions developed in this study, a better understanding of the effects of in situ aging and moisture damage on the stiffness, fatigue, and permanent deformation properties of the mix is needed.

• The desirability of compacting specimens in the laboratory using methods that duplicate in situ aggregate orientation, aggregate interparticle contact, and asphalt-aggregate interfaces is acknowledged. The rolling wheel compactor used in this study allowed the preparation of both fatigue beams and RSST-CH specimens with performance characteristics similar to those produced by field compaction.

• The permanent deformation analysis procedure demonstrated in this study produced results that follow engineering expectations and correlated well with available field data. In all cases, results were somewhat conservative.

• The fatigue analysis procedure demonstrated in this study showed that fatigue life and flexural stiffness must be evaluated together within a mechanistic analysis of the pavement in order to determine the best mix for a project. The mechanistic analysis used in this study, linear elastic layer theory, can be improved upon, but the need for mechanistic analysis to determine the best mix for a given project is clear.

• Confining pressures of up to 68.9 kPa (10 psi) have little or no effect on RSST-CH results. To evaluate permanent shear deformation for the mix design of dense-graded mixes, it is recommended that specimens be compacted to the minimum air-void content expected in the field after traffic densification, approximately 3.0 percent (measured using parafilm) for most dense-graded mixes. Little data have been evaluated regarding critical air-void contents for open-graded mixes. It is recommended that specimens for these mixes be compacted to the air-void content expected after densification caused by initial trafficking.

ACKNOWLEDGMENTS

The authors thank the Institute of Transportation Studies, University of California at Berkeley (UCB) for its support of this study. The kind help of the following agencies, companies, and individuals is also greatly appreciated: California Department of Transportation (TransLab and District 8 Laboratory and Maintenance crews), Wisconsin Department of Transportation, Joseph Vicelja, the Strategic Highway Research Program, Nichols Consulting Engineers, Akhtar Tayebali, Daniel Sosnovske, and the laboratory staff at the UCB Asphalt Research Program.

REFERENCES

1. Sousa, J., A. Tayebali, J. Harvey, P. Hendricks, and C. L. Monismith: Sensitivity of SHRP A-003A Proposed Testing Equipment to Mix Design Parameters for Permanent Deformation and Fatigue. In *Transportation Research Record 1384,* TRB, National Research Council, Washington, D.C., 1993.
2. Tayebali, A., J. Deacon, J. Coplantz, J. Harvey, and C. L. Monismith. Mixture and Mode-of-Loading Effects on Fatigue Response of Asphalt-Aggregate Mixtures. Presented at the Annual Meeting of the Association of Asphalt Paving Technologists, 1994.
3. Harvey, J., and C. L. Monismith. Effects of Laboratory Asphalt-Concrete Specimen Preparation Variables on Fatigue and Permanent Deformation Test Results Using SHRP A-003A Proposed Testing Equipment. In *Transportation Research Record 1417,* TRB, National Research Council, Washington, D.C., 1993.
4. *Standard Practice for Preparation of Bituminous Mixture Test Specimens by Means of Rolling Wheel Compactor.* Interim Proposed Standard Practice Specification. SHRP A-003A, Washington, D.C., May 12, 1992.
5. Harvey, J., J. Sousa, J. Deacon, and C. L. Monismith. Effects of Sample Preparation and Air-Void Content on Asphalt Concrete Properties. In *Transportation Research Record 1317,* TRB, National Research Council, Washington, D.C., 1991.
6. Sousa, J. Asphalt-Aggregate Mix Design Using the Simple Shear Test (Constant Height). Presented at the Association of Asphalt Paving Technicians Annual Meeting, 1994.
7. Solaimanian, M., and T. Kennedy. Predicting Maximum Pavement Surface Temperature Using Maximum Air Temperature and Hourly Solar Radiation. In *Transportation Research Record 1417,* TRB, National Research Council, Washington, D.C., 1993.
8. Harvey, J., C. L. Monismith, and J. Sousa. An Investigation of Field- and Laboratory-Compacted Asphalt-Rubber, SMA, Recycled and Conventional Asphalt-Concrete Mixes Using SHRP A-003A Equipment. Presented at the Association Annual Meeting of Asphalt Paving Technicians 1994.
9. Deacon, J. A., A. A. Tayebali, J. S. Coplantz, F. N. Finn, and C. L. Monismith. *Fatigue Response of Asphalt-Aggregate Mixtures, Part III—Mixture Design and Analysis.* Prepared for Strategic Highway Research Program, Project A-003A. Institute of Transportation Studies, University of California, Berkeley, May 1993.
10. Sousa, J., and M. Solaimanian. Abridged Procedure to Determine Permanent Deformation of Asphalt Concrete Pavements. Presented at the 73rd Annual Meeting of the Transportation Research Board, Washington, D.C., 1994.
11. Sousa, J., et al. *Permanent Deformation Response of Asphalt-Aggregate Mixes.* Prepared for Strategic Highway Research Program, Project A-003A. Institute of Transportation Studies, University of California, Berkeley, March 1994.

The views expressed in this paper are those of the authors and do not necessarily reflect those of the agencies, companies, or individuals who supported the study.

Publication of this paper sponsored by Committee on Characteristics of Bituminous Paving Mixtures To Meet Structural Requirements.